DOI: 10.1093/brain/awh088 *Brain* (2004), **127,** 791–800

Cerebral atrophy in Parkinson's disease with and without dementia: a comparison with Alzheimer's disease, dementia with Lewy bodies and controls

Emma J. Burton,[1] Ian G. McKeith,[1] David J. Burn,[2] E. David Williams[3] and John T. O'Brien[1]

[1]*The Institute for Ageing and Health, University of Newcastle upon Tyne,* [2]*Department of Neurology, Regional Neurosciences Centre, Newcastle General Hospital, Newcastle, and* [3]*Regional Medical Physics Department, Sunderland Royal Hospital, Sunderland, UK*

Correspondence: Dr Emma J Burton, Institute for Ageing and Health, Wolfson Research Centre, Newcastle General Hospital, Westgate Road, Newcastle upon Tyne NE4 6BE, UK
E-mail: e.j.burton@ncl.ac.uk

Summary

Parkinson's disease is a common neurodegenerative disorder primarily characterized by rigidity, tremor and bradykinesia. Cognitive impairment and neuropsychiatric symptoms are frequent in Parkinson's disease, with a 70% cumulative incidence of dementia. The aim of this cross-sectional study was to establish the pattern of cerebral atrophy on MRI in Parkinson's disease patients with dementia. We used voxel-based morphometry (VBM) to provide an unbiased means of investigating brain volume loss. Whole brain structural T1-weighted MRI scans from Parkinson's disease patients with dementia (PDD, *n* = 26), Parkinson's disease patients without dementia (*n* = 31), Alzheimer's disease patients (*n* = 28), patients with dementia with Lewy bodies (DLB, *n* = 17) and control subjects (*n* = 36) were acquired. Images were analysed using SPM99 and the optimized method of VBM. Reduced grey matter volume in PDD patients compared with controls was observed bilaterally in the temporal lobe, including the hippocampus and parahippocampal gyrus, and in the occipital lobe, the right frontal lobe and the left parietal lobe, as well as some subcortical regions. Parkinson's disease patients without dementia showed reduced grey matter volume in the frontal lobe compared with control subjects. There was significant grey matter atrophy bilaterally in the occipital lobe of PDD patients compared with Parkinson's disease patients. In addition, significant temporal lobe atrophy, including the hippocampus and parahippocampal gyrus was detected in Alzheimer's disease relative to PDD. No significant volumetric differences were observed in PDD compared with DLB. Thus, Parkinson's disease involves grey matter loss in frontal areas. In PDD, this extends to temporal, occipital and subcortical areas, with occipital atrophy in PDD being the only difference between the two groups. This provides important information about the pattern of cerebral atrophy in Parkinson's disease and PDD.

Keywords: Parkinson's disease; voxel-based morphometry; MRI; dementia; atrophy

Abbreviations: BA = Brodmann area; CAMCOG = Cambridge Cognitive Examination; DLB = dementia with Lewy bodies; FWHM = full width at half maximum; MMSE = Mini-Mental State Examination; MNI = Montreal Neurological Institute; PDD = Parkinson's disease with dementia; ROI = region of interest; SPM = statistical parametric mapping; TIV = total intracranial volume; UPDRS III = Unified Parkinson's Disease Rating Scale III; VaD = vascular dementia; VBM = voxel-based morphometry.

Received July 23, 2003. Revised November 11, 2003. Accepted December 1, 2003 Advance Access publication January 28, 2004

Introduction

Parkinson's disease is a common neurodegenerative disorder, affecting 1% of people over 65 years. Incidence studies suggest that the risk of developing dementia in Parkinson's disease is ~70% and almost 6-fold that of age-matched controls (Aarsland *et al.*, 2001). The clinical picture of dementia in Parkinson's disease (PDD), with visual hallucinations and fluctuating confusion, closely resembles that of dementia with Lewy bodies (DLB). Current consensus criteria for DLB, however, suggest that distinction is made between the two conditions, based solely on the duration of

the extrapyramidal symptoms. Diagnostically, PDD subjects are thus arbitrarily identified as those patients having motor symptoms for a 12-month period or more prior to the development of features of DLB, the diagnosis being DLB if the dementia develops within 12 months of motor symptoms.

There is a need to determine the biological substrates underlying PDD and the extent to which these are the same as in DLB. Apaydin *et al*. (2002) found, neuropathologically, that patients with Parkinson's disease who develop dementia had a 10-fold increase in Lewy body counts in the neocortex and limbic areas compared with PDD. PDD, like DLB, is associated with cortical cholinergic loss and increasingly evidence points to the efficacy of cholinesterase inhibitors in both disorders (Reading *et al*., 2001; Aarsland *et al*., 2002). Structural MRI studies have potential to provide important insights into the relationship between PDD, DLB and Alzheimer's disease. Most studies have focused on Alzheimer's disease, identifying temporal lobe and hippocampal atrophy compared with controls and a brain atrophy rate associated with increasing severity of cognitive decline (O'Brien *et al*., 2001). DLB is also associated with generalized atrophy and ventricular enlargement but, in contrast to Alzheimer's disease, has less marked changes in the medial temporal lobe and hippocampus (Barber *et al*., 2000; Burton *et al*., 2002).

Previous MRI studies found no evidence of generalized atrophy and ventricular enlargement in Parkinson's disease compared with controls (Huber *et al*., 1989). In addition, Schulz *et al*. (1999) reported that striatal brainstem and cerebeller volumes are normal in idiopathic Parkinson's disease. More sensitive MRI methods have, however, shown significant increases in annual brain volume loss in non-demented Parkinson's disease patients compared with control subjects (Hu *et al*., 2001), with atrophy of the medial temporal lobe structure in Parkinson's disease being similar to that of Alzheimer's disease (Double *et al*., 1996).

An early study of PDD did not find any particular pattern of abnormality on MRI (Huber *et al*., 1989). In contrast, the annual rate of brain atrophy has recently been correlated with global cognitive decline (Hu *et al*., 2001), supported by findings of diffuse cerebral atrophy and basal ganglia degeneration in Parkinson's disease patients with cognitive impairment (Alegret *et al*., 2001). Hippocampal atrophy may not be specific to Alzheimer's disease but also occurs in vascular dementia (VaD) (Barber *et al*., 2000) and Parkinson's disease with and without dementia (Laakso *et al*., 1996; Camicioli *et al*., 2003). Laakso *et al*. (1996) reported that raw hippocampal volumes in PDD were smaller than those in Alzheimer's disease (but not significantly so) and that the volume in Parkinson's disease patients without dementia was diminished to a lesser extent. In, Parkinson's disease, hippocampal volume reduction has been linked to memory impairment (Riekkinen *et al*., 1998).

Frontal lobe atrophy has also been described as a feature of both late-onset Parkinson's disease and DLB, while frontal lobe atrophy correlates with duration of motor symptoms (Double *et al*., 1996). Frontal lobe changes would be consistent with the prominent executive impairment, characteristic of Parkinson's disease with early cognitive impairment and PDD (Owen *et al*., 1999).

Most previous studies on Parkinson's disease have concentrated on visual inspection or region of interest (ROI) based methods. ROI analyses are operator dependent and rely on the arbitrary nature of boundary choice to define a structure, as well as predefining the structure to be investigated. Automated unbiased voxel-based methods enable analysis of the whole brain in an operator-independent environment. Voxel-based morphometry (VBM) has been implemented in various studies of dementia including Alzheimer's disease (Rombouts *et al*., 2000; Baron *et al*., 2001; Karas *et al*., 2003), DLB (Burton *et al*., 2002) and Parkinson's disease (Kassubek *et al*., 2002).

In this study, we used VBM to study the pattern of cerebral atrophy in Parkinson's disease with and without dementia in comparison to normal controls, Alzheimer's disease and DLB. We hypothesized that brain atrophy would be greater in PDD than in Parkinson's disease, and that the pattern would be more similar to that seen in DLB than in Alzheimer's disease.

Methods

Subjects

The sample consisted of 159 subjects (34 with Parkinson's disease, 31 with PDD, 20 with DLB, 35 with Alzheimer's disease and 39 healthy elderly controls). Subjects underwent MRI scans as part of a baseline assessment in a prospective longitudinal study of dementia. Patients entering this study were selected from hospital and community dwelling populations under the care of local consultant old age psychiatrists, geriatricians and neurologists. Control subjects were recruited from friends and spouses of patients or carers. The Newcastle and North Tyneside ethics committee approved the study. All subjects gave informed consent to participate.

Assessments and diagnosis

Subjects underwent detailed physical, neurological and neuropsychiatric examinations, which included clinical history, mental state and physical examination and, for demented subjects, a standard blood screen with thyroid function tests, B12, folate and syphilis serology, and CT scan. Standardized schedules administered included the Mini-Mental State Examination (MMSE) (Folstein *et al*., 1975), the Cambridge Cognitive Examination (CAMCOG) (Roth *et al*., 1986), the Neuropsychiatric Inventory (NPI) (Roth *et al*., 1986) and the motor subsection of the Unified Parkinson's Disease Rating Scale III (UPDRS III) (Fahn *et al*., 1987). Diagnosis was made by consensus between experienced clinicians using the National Institute of Neurological and Communicative Disorders and Stroke/Alzheimer's Disease and Related Disorders Association (NINCDS/ADRDA) criteria for Alzheimer's disease (McKhann *et al*., 1984), the consensus criteria for DLB and PDD (McKeith *et al*., 1996) and the UK Parkinson's Disease Society Brain Bank criteria for Parkinson's disease (Gibb and Lees, 1988). All Alzheimer's disease subjects met criteria for probable Alzheimer's disease, 18 DLB subjects fulfilled probable and two possible DLB

Table 1 *Demographic and neuropsychological data of subjects studied with MRI*

	Control (n = 36)	Parkinson's disease (n = 31)	PDD (n = 26)	Alzheimer's disease (n=28)	DLB (n = 17)	P value
Sex (M:F)	20:16	23:8	16:10	14:14	9:8	NS
Age	75.1 ± 6.6	75.2 ± 5.2	72.3 ± 5.2	77.9 ± 5.4	75.5 ± 7.2	0.007*
MMSE (max 30)	28.1 ± 1.6	26.4 ± 1.9	18.9 ± 5.8	18.8 ± 4.6	16.5 ± 6.1	0.0001**
CAMCOG (max 107)	93.6 ± 4.0	87.6 ± 8.4	63.9 ± 16.9	64.7 ± 13.2	61.1 ± 15.5	0.0001**
Total UPDRS III (max 108)	1.2 ± 1.9	25.8 ± 11.1	36.4 ± 10.5	4.0 ± 3.8	26.8 ± 16.9	0.001†
Duration of illness (months)	NA	43.5 ± 34.2	82.0 ± 60.6	31.8 ± 17.2	28.6 ± 16.7	0.001††

Values expressed as mean ± SD. Gabriel's *post hoc* tests: *Alzheimer's disease > PDD; **control and Parkinson's disease > Alzheimer's disease, DLB, PDD; (NB Alzheimer's disease versus DLB, PDD and control versus Parkinson's disease = NS). Mann–Whitney *post hoc* tests: †Alzheimer's disease, DLB, Parkinson's disease, PDD > control; DLB > Alzheimer's disease; PDD > Alzheimer's disease, Parkinson's disease; (NB DLB versus Parkinson's disease and PDD versus DLB = NS); ††PDD > Parkinson's disease, DLB, Alzheimer's disease (NB DLB versus Alzheimer's disease = NS; and Parkinson's disease versus Alzheimer's disease, DLB = NS). NA = not applicable; NS = not significant.

criteria, while all Parkinson's disease and PDD subjects met the clinical diagnostic criteria for Parkinson's disease. In addition, all PDD subjects met criteria for probable DLB, which had developed ⩾12 months after the onset of motor symptoms.

Neuroimaging and data analysis

All scans were performed on a 1.5 Tesla GE Signa scanner (General Electric, Milwaukee, WI, USA). Whole brain T1-weighted 3D FSPGR data sets were acquired in the coronal plane [TR (repetition time) = 12.4 ms, TE (echo time) = 4.2 ms, TI (inversion time) = 650 ms, 256 × 256 matrix, 1.6 mm slice thickness, flip angle = 15°, FOV (field of view) = 20 cm, in plane resolution 0.78 × 0.78 mm] yielding 124 contiguous slices through the head. Standard head positioning was used throughout.

Images were transferred to a personal computer and converted to Analyze format using Mricro (http://www.mricro.com) and subsequently transferred to a Sun Ultra 30 workstation (Sun Microsystems Inc., Mountainview, CA, USA) and analysed using SPM99 (Statistical Parametric Mapping, Wellcome Department of Cognitive Neurology, London, UK; http//www.fil.ion.ucl.ac.uk/spm) and Matlab 5.3.1 (The Mathworks, MA, USA). The optimized VBM protocol was applied to the images (Good *et al*., 2001). Prior to image analysis, all images were checked for movement artefacts and manually re-orientated using the reorient function of SPM99, so that they were centred on the anterior commissure. Those images degraded by movement were excluded from further analyses, leaving a total study cohort, comprising 17 DLB, 28 Alzheimer's disease, 26 PDD, 31 Parkinson's disease and 36 controls.

VBM

Templates

Customized whole brain and grey matter templates were created in order to facilitate optimal normalization and segmentation of elderly patient and control MRI scans. Templates were constructed for each comparison and included data from all subjects in the groups involved in that specific comparison, in an attempt to reduce the potential for bias towards one group during spatial normalization (Ashburner and Friston, 2000). To construct the customized whole brain template, the original images were spatially normalized to the T1 Montreal Neurological Institute (MNI) template, which approximates the space defined by Talairach and Tournoux (1988) without

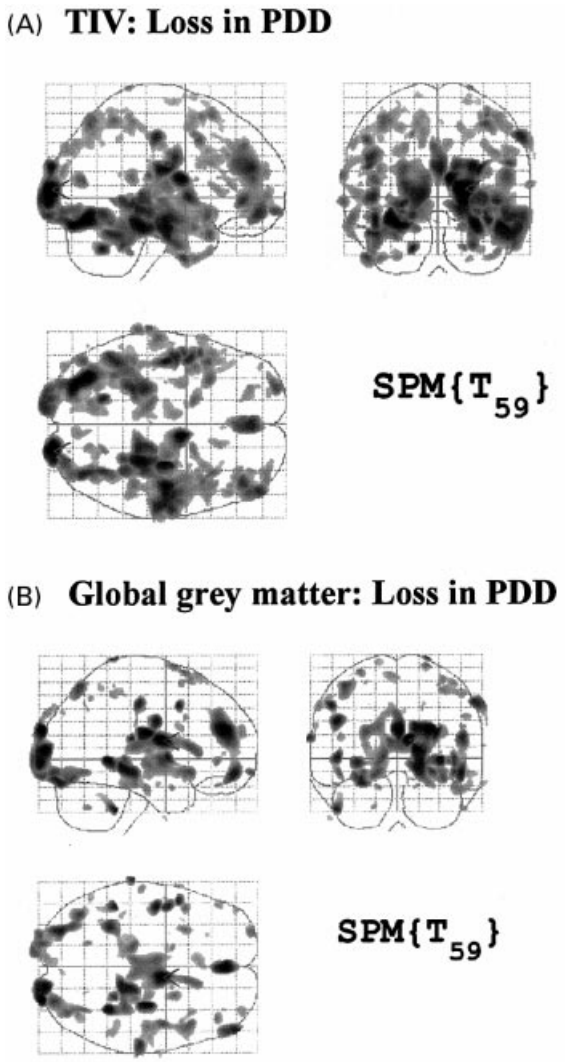

Fig. 1 The effects of modelling global volume for the analysis of PDD relative to controls. Atrophy in PDD shown (**A**) compensated for differences in head size, with significant changes in the temporal, occipital and frontal lobes and subcortical regions at $P < 0.001$ uncorrected, and (**B**) as regional changes in grey matter, above that occurring globally, with significant changes in the thalamus, caudate and occipital lobe at $P < 0.01$ uncorrected.

Table 2 *Location and Talairach coordinates of significant clusters of grey matter volume loss on PDD compared with controls when TIV was included in the analysis*

$P_{corrected}$	Cluster (k)	Talairach coordinates			Location
		x	y	z	
0.000	38364	–33	–70	–11	L occipital lobe fusiform 19
		–45	–15	–13	L temporal lobe subgyral 21
		–47	2	0	L superior temporal lobe 22
		–25	–30	–16	L parahippocampal gyrus
		–48	–53	–19	L temporal lobe fusiform 37
		–26	–38	–2	L hippocampus
		–19	–99	10	L occipital lobe cuneus 18
		–24	–96	14	L middle occipital gyrus 19
		–26	–94	23	L middle occipital gyrus 18
		–45	15	–11	L superior temporal gyrus 38
		–16	4	–19	L uncus
		–24	–82	37	L occipital lobe cuneus 19
		–42	–84	23	L superior occipital lobe 19
0.000	44909	9	–3	13	R thalamus
		27	–34	–15	R parahippocampal gyrus
		46	–14	–17	R subgyral 20
		30	–14	20	R claustrum
		58	–18	–18	R inferior temporal lobe 21
		60	–11	–11	R middle temporal lobe 21
		32	–30	2	R caudate tail
		55	–8	–28	R inferior temporal lobe 20
		49	–16	–2	R superior temporal lobe 22
		40	–20	–6	R insula
		23	–13	10	R putamen
		30	–9	–9	R amygdala
		45	17	–9	R inferior frontal lobe 47
		46	7	–13	R superior temporal gyrus 38
		38	–10	25	R insula
		47	–31	–11	R temporal lobe fusiform 20
0.000	8466	43	40	–5	R middle frontal lobe 47
		50	46	12	R inferior frontal lobe 46
		40	56	–2	R middle frontal lobe 10
		34	45	1	R subgyral
0.001	6047	–3	41	31	L medial frontal lobe 9
0.005	4269	–28	–60	49	L superior parietal lobe 7
		–25	–40	60	L postcentral gyrus 5
		–53	–38	46	L inferior parietal lobe 40

A threshold of $P < 0.01$ (cluster level corrected) was used to identify the most significant peaks. Coordinates (x, y, z) refer to standard Talairach space (Talairach and Tournoux, 1988). Results are listed by cluster size as indicated by the value k, the number of voxels in a particular cluster. Numbers refer to Brodmann areas (location). L = left; R = right.

any non-linear registration. Subsequently, the normalized scans were averaged and the resulting mean image was smoothed with an 8-mm full width at half maximum (FWHM) Gaussian kernel. The creation of study-specific grey matter templates involved spatially normalizing all structural images to the customized whole brain template, segmentation into grey matter, white matter and CSF partitions, brain extraction (for removing non-brain voxels from the grey matter images) and smoothing with an 8-mm FWHM kernel. The smoothed grey matter images were then averaged to create a grey matter template. This template was created to optimize the spatial normalization to grey matter and, by including the images as prior probability maps in the segmentation, permitted optimized segmentation and reduced the potential bias introduced when probability maps from young healthy controls are used.

Optimized VBM

Following the creation of study specific grey matter templates, the optimized protocol was subsequently applied to the original data (Good *et al*., 2001, 2002). Briefly, the original structural images were segmented in native space and extracerebral voxels were removed from the grey matter segments by a fully automated procedure. The 'brain extract' function involves a series of morphological operations (erosions and dilations) to remove non-cerebral regions (skull,

Table 3 *Location and Talairach coordinates of significant clusters of grey matter volume loss in PDD compared with controls when mean grey matter global was modelled as a covariate*

$P_{corrected}$	Cluster (*k*)	Talairach coordinates			Location
		x	*y*	*z*	
0.002	15087	8	–2	14	R thalamus
		16	–33	–4	R parahippocampal gyrus
		32	–31	1	R caudate
		–5	–6	13	L thalamus
		12	20	7	R thalamus (medial dorsal nucleus)
		14	24	4	R caudate
		–3	–19	13	L thalamus

Notes as for Table 2.

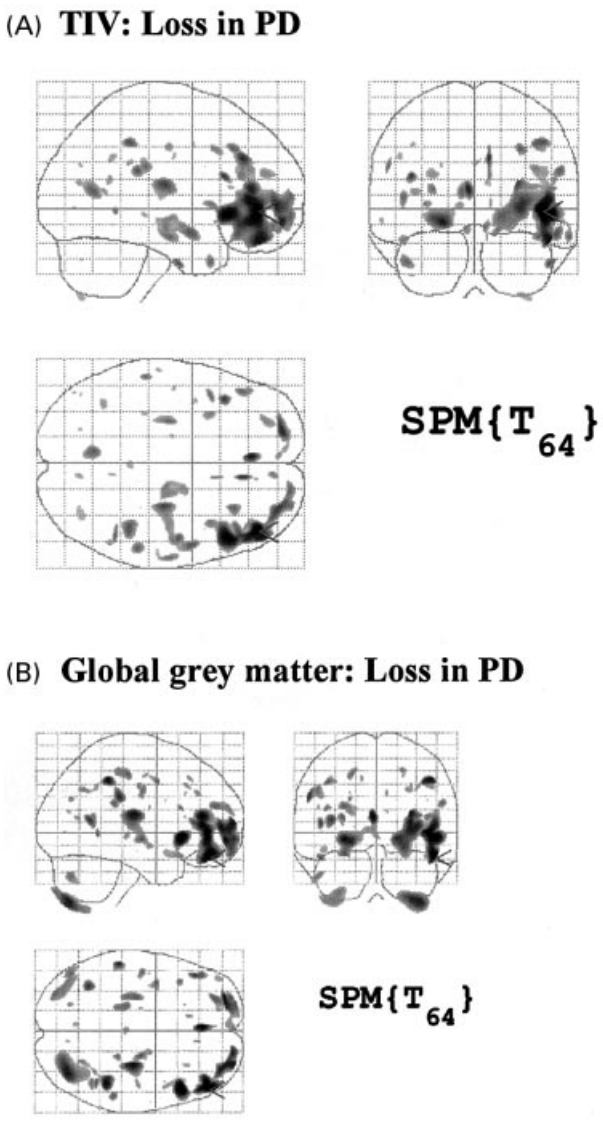

Fig. 2 Atrophy in Parkinson's disease patients shown (**A**) compensated for differences in head size, with significant grey matter loss observed in the right frontal lobe at $P < 0.001$ uncorrected, and (**B**) as regional changes in grey matter, above that occurring globally, with less significant changes in the right frontal lobe at $P < 0.01$ uncorrected.

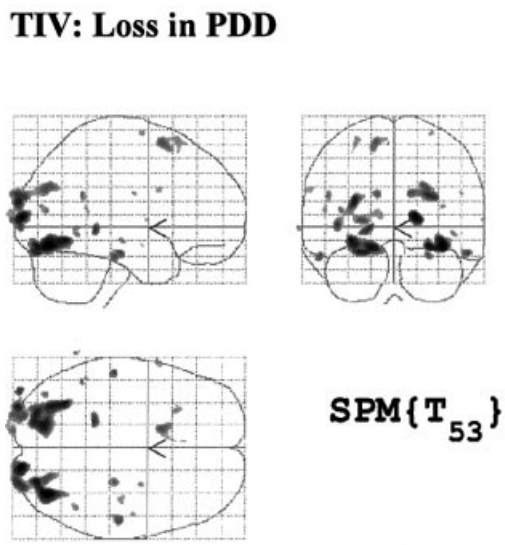

Fig. 3 Grey matter volume loss in PDD relative to Parkinson's disease, accounting for differences in head size ($P < 0.001$ uncorrected). Atrophy was observed in the occipital lobe bilaterally, although less significant on the right.

scalp and other non-brain tissue) from the segmentations. The extracted grey matter images were then normalized to the customized grey matter template (created previously) using a 12-parameter affine transformation and non-linear iterations to account for global non-linear shape differences (Ashburner and Friston, 1999). The normalization parameters were subsequently reapplied to the original whole brain structural images, which were then resliced to a voxel size of 1 mm^3. The normalized whole brain images were then automatically segmented into grey matter, white matter, CSF and other non-brain tissue using a modified clustering algorithm based on the relative distribution of tissue types and using the customized prior probability maps. A correction for inhomogeneity was incorporated in the segmentation process. Again, the 'brain extract' routine was used to remove any remaining extracerebral tissue from the grey matter segments. The resulting grey matter images were 'modulated' in order to preserve the volume of a particular tissue compartment within each voxel. Modulation is a process in which information from the deformation field generated during spatial normalization is used to render the VBM analysis more comparable to ROI analysis. The modulated images were smoothed with a 10-mm FWHM

Table 4 *Grey matter volume loss in Parkinson's disease relative to controls with TIV included. Location and Talairach coordinates of significant clusters are presented*

$P_{corrected}$	Cluster (k)	Talairach coordinates			Location
		x	y	z	
0.000	10670	44	41	–3	R frontal lobe subgyral 10
		49	22	–4	R inferior frontal gyrus 47
		47	37	3	R inferior frontal gyrus 45
		30	53	–2	R superior frontal gyrus 10
		18	61	–6	R medial frontal gyrus 10
		28	61	4	R superior frontal gyrus
		37	12	2	R insula
		37	37	22	R middle frontal gyrus 10

Notes as for Table 2.

Table 5 *Grey matter volume loss in PDD relative to Parkinson's disease. Location and Talairach coordinates of significant clusters are presented for analysis with TIV*

$P_{corrected}$	Cluster (k)	Talairach coordinates			Location
		x	y	z	
0.004	4364	–32	–60	–5	L occipital lingual gyrus 19
		–16	–75	–10	L occipital lingual gyrus 18
		–30	–38	–7	L occipital fusiform gyrus 19

Notes as for Table 2.

isotropic Gaussian kernel to render the data ready for statistical analysis by conditioning the residuals to conform to the Gaussian random field model (Friston *et al*., 1995). The resulting smoothed, modulated, normalized regions contained the average amount of grey matter within a region surrounding a voxel. This enabled the investigation of the absolute volume of grey matter (Ashburner and Friston, 2000; Good *et al*., 2001).

Statistical analysis

The smoothed, modulated grey matter data were analysed using statistical parametric mapping (SPM99) employing the General Linear Model (Friston *et al*., 1995). Volumetric changes in grey matter were tested by analysis of the modulated data. Since, during modulation, we incorporated the correction for volume change induced by spatial normalization, it was appropriate to include total intracranial volume (TIV) as a covariate to remove any variance due to differences in head size. TIV was calculated using the 'get_globals' function of SPM99. The number of voxels in each of the tissue compartments was calculated and summed. Global grey matter voxel intensity was included as a covariate to determine the regionally specific pattern of loss within the grey matter compartment, over and above global or generalized grey matter change.

Two-tailed contrasts were constructed to examine both increases and decreases in grey matter between two groups. The analysis of covariance was used when TIV and mean grey matter globals were included in the analysis. The statistical parametric maps were thresholded at $P < 0.001$ uncorrected for multiple comparisons and all images are presented in neurological orientation (i.e. right of the images is right side of brain, unless otherwise stated). The coordinates of peak voxels were transferred from MNI space to Talairach space using a non-linear transform approach described by Brett *et al*. (1999). The Talairach daemon (Lancaster *et al*., 2000) was used for anatomical localization of changes.

Results

Demographics

Table 1 shows the demographic and clinical characteristics of all groups. Groups were matched for sex and broadly matched for age, although the Alzheimer's disease group were older than the PDD ($P < 0.007$) group. As anticipated, MMSE and CAMCOG scores were lower in all dementia groups than in controls and cognitively intact Parkinson's disease subjects ($P < 0.001$). There were no significant differences in global cognitive measures between the control and Parkinson's disease groups or between the three dementia groups. The DLB, Parkinson's disease and PDD groups had higher UPDRS III scores than both Alzheimer's disease patients and normal controls ($P < 0.001$), with Alzheimer's disease patients having higher scores than controls $P < 0.001$). There were no significant differences in UPDRS III scores between DLB and Parkinson's disease groups. PDD subjects had higher UPDRS scores and a longer duration of illness than any of the other patients groups ($P < 0.001$).

VBM results

Figure 1A demonstrates atrophy detected by VBM, covarying for TIV, in PDD relative to controls. PDD patients had a relatively diffuse pattern of grey matter volume loss bilat-

erally in the temporal [Brodmann area (BA) 20, 21, 22, 37, 38, 41 and 42] and occipital (BA 18 and 19) lobe areas as well as the middle and inferior frontal gyri (BA 9, 10, 46, 47) on the right ($P < 0.0001$). Although less marked, changes were also observed in left inferior and superior parietal lobes (BA 5 and 7) ($P < 0.005$ corrected). Subcortical areas showing significant losses included the caudate tail and putamen on the right and the thalamus bilaterally ($P < 0.0001$). To determine regionally specific patterns of loss in the grey matter compartment itself, mean global grey matter was included. In PDD, atrophy (thresholded as $P < 0.01$ uncorrected) was seen in the thalamus bilaterally and in the right caudate (Fig. 1B). Tables 2 and 3 show the location and Talairach coordinates for results obtained from analysis with TIV and mean grey matter, respectively, comparing PDD patients with controls. Examination of the reverse contrast did not yield any significant results (i.e. there were no grey matter volume increases in PDD compared with controls).

Parkinson's disease patients without cognitive impairment showed significant clusters of reduced grey matter volume compared with controls, in the superior, middle and inferior frontal gyri (BA 10, 45, 47) on the right (Fig. 2A). The pattern of grey matter atrophy was similar, although less significant with grey matter globals included as a covariate (thresholded at $P < 0.01$ uncorrected) (Fig. 2B). There were no grey matter volume increases in Parkinson's disease relative to controls. Table 4 contains information regarding the location and Talairach coordinates of significant regions.

Comparing PDD with Parkinson's disease, there was significant grey matter loss in the fusiform and lingual gyri of the left occipital lobe (BA 18 and 19) and less significantly in the same areas on the right ($P < 0.047$ corrected) (Fig. 3 and Table 5). No regionally specific grey matter change was observed beyond the global grey matter change. No significant grey matter losses (globally or regionally) were observed in the Parkinson's disease patients relative to PDD.

Compared with Alzheimer's disease, PDD patients showed no significant grey matter volume loss. In Alzheimer's disease relative to PDD, significant atrophy was observed in the hippocampus and parahippocampal gyrus bilaterally, and in the inferior temporal gyrus (BA 20), claustrum and right uncus (BA 28) (Fig. 4A). A similar pattern of atrophy was observed when mean grey matter globals were included to look at regional changes (Fig. 4B).

There was no difference in grey matter atrophy between PDD and DLB, irrespective of whether TIV or mean grey matter globals were included. Similar results from all the analyses were obtained when the two possible DLB cases were excluded.

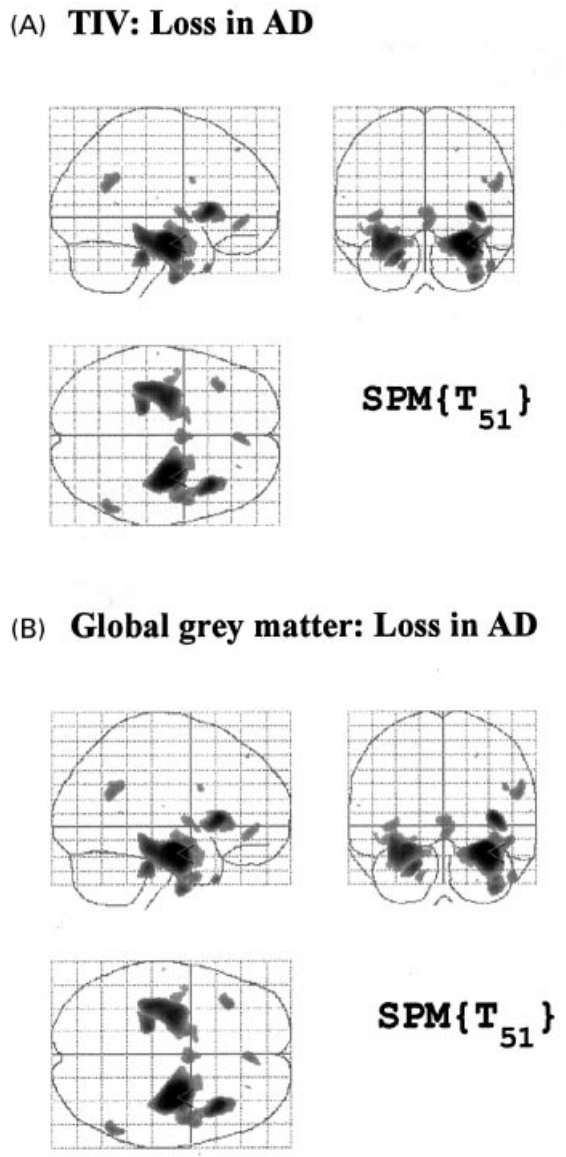

Fig. 4 Atrophy in Alzheimer's disease patients shown (**A**) compensated for differences in head size and (**B**) as regional changes in grey matter, above that occurring globally presented at $P < 0.001$. There is significant grey matter volume reduction bilaterally in the hippocampus, parahippocampal gyrus and inferior temporal lobe.

Discussion

Using VBM, we have shown that Parkinson's disease patients have significant reductions in grey matter volume in the frontal and temporal lobes compared with control subjects. This is in agreement with previous studies, which have reported diffuse gyral atrophy throughout the temporal, parietal and frontal cortices (Hu *et al*., 2001). Decreased frontal lobe perfusion has also been observed in Parkinson's disease with and without dementia, with greater perfusion deficits in those with dementia (Antonini *et al*., 2001).

Although early MRI studies in PDD suggested that there was no distinct pattern of atrophy on MRI (Huber *et al*., 1989), more recently it has been suggested that the atrophy observed in PDD is not only different to Parkinson's disease without dementia but that it takes a similar form to Alzheimer's disease, affecting the medial temporal lobe (Laakso *et al*., 1996). Our results, however, suggest that the

Table 6 *Grey matter volume loss in Alzheimer's disease relative to PDD. Location and Talairach coordinates of significant clusters are presented for analysis with TIV and mean grey matter*

$P_{corrected}$	Cluster (*k*)	Talairach coordinates			Location
		x	*y*	*z*	
TIV					
0.0001	13744	31	–11	–15	R parahippocampal gyrus
		37	–8	–37	R inferior temporal gyrus 20
		48	–3	–9	R temporal lobe subgyral 21
		38	–10	–7	R claustrum
		22	5	–21	R uncus 28
0.0001	9084	–27	–13	–14	L hippocampus
		–35	–26	–14	L parahippocampal gyrus
		–17	1	–15	L parahippocampal gyrus
		–12	2	–16	L frontal lobe subcallosal
		–21	–30	–7	L parahippocampal gyrus
Mean global grey matter					
0.0001	9304	30	–11	–15	R hippocampus
		38	–10	–7	R claustrum
		48	–3	–9	R temporal subgyral
		22	5	–21	R uncus
0.0001	6581	–26	–13	–14	L hippocampus
		–35	–27	–14	L parahippocampal gyrus

Notes as for Table 2.

pattern of grey matter volume loss in PDD is different from Alzheimer's disease and resembles more closely the pattern of atrophy observed in DLB. When global grey matter was modelled, atrophy of the thalamus and caudate was observed, which suggests that atrophy in these structures exceeds that for grey matter in general in patients with PDD. Recent studies have highlighted the α-synuclein burden in striatum (Duda *et al*., 2002) and thalamic nuclei (Rüb *et al*., 2002), providing a plausible pathological substrate for these findings.

We also found greater hippocampal atrophy in Alzheimer's disease than in PDD, which is contrary to some previous reports (Laakso *et al*., 1996), although in agreement with others (Camicioli *et al*., 2003). Laakso *et al*. (1996) reported that the absolute volume of the hippocampi in PDD was smaller than that of Alzheimer's disease patients, although not significantly so, while the coexistence of Alzheimer's disease pathology in the Parkinson's disease group could not be ruled out. In a recent study of MCI (mild cognitive impairment) patients, hippocampal and infero-lateral temporal atrophy was observed when compared with controls (Chetelat *et al*., 2002). This was in contrast to the more superior and posterior regions affected in Alzheimer's disease. In a recent VBM study, frontotemporal dementia was reported to be associated with dorsolateral atrophy while semantic dementia showed bilateral anterior temporal and hippocampal atrophy (Rosen *et al*., 2002). In a comprehensive ROI study, asymmetric hippocampal atrophy was found to be more extensive in semantic dementia than Alzheimer's disease (Galton *et al*., 2001). This finding was confirmed by others (Chan *et al*., 2001). However, Mummery *et al*. (2000) reported temporal pole, inferolateral temporal lobe and ventromedial frontal atrophy but failed to detect hippocampal atrophy in semantic dementia. We included in our PDD group only subjects who fulfilled DLB criteria (i.e. had additional symptoms of fluctuation and/or hallucinations) and did not include subjects with a progressive steady cognitive decline in the absence of these features. Since the latter might be more similar to the clinical profile of Alzheimer's disease, our sample was possibly biased against the inclusion of Parkinson's disease subjects who might also have Alzheimer's disease pathology and hippocampal changes. One potential limitation of our study is the reliance on clinical, rather than autopsy proven, diagnoses. However, we used the most specific and best validated (against autopsy) currently available and our centre is one of the few to verify its clinical diagnoses of Alzheimer's disease and DLB against autopsy (McKeith *et al*, 2000).

The reduced grey matter volume observed in the occipital lobe in PDD was contrary to previous findings. The only difference between Parkinson's disease groups with and without dementia was grey matter loss in the right occipital lobe of the PDD group. Occipital hypoperfusion in Parkinson's disease patients without dementia has been reported and is correlated with impaired cortical visual processing (Abe *et al*., 2003). Whether this hypoperfusion is associated with structural change is unclear. Occipital hypoperfusion is a recognised feature of DLB (Colloby *et al*., 2002), but using both ROI (Middelkoop *et al*., 2001) and VBM (Burton *et al*., 2002) approaches we previously

showed that this did not appear secondary to occipital lobe atrophy (Middelkoop *et al*., 2001). Uncertainty remains, therefore, as to the relationship between atrophy, neuropathology and perfusion deficits in Parkinson's disease with and without dementia.

VBM is not without its limitations. Spatial normalization is used to map each image to a template image in standard space. In order to reduce the degree of non-linear warping, we used customized T1 templates created from controls and patients. By spatially normalizing the data, there is the potential to introduce errors which can show regional specificity, especially were variance is high. Small structures such as the hippocampus show high variability among the elderly and diseased groups. VBM may be insensitive to the detection of subtle changes/atrophy in areas of high variance, although VBM detected atrophy of the hippocampus has been demonstrated previously. Image segmentation is fully automated, but is subject to potential partial volume effects, particularly at the interface between tissue types. This effect may be increased in diseased or elderly brains where the tissue contrast is reduced and may lead to misclassification of voxels. In an attempt to reduce the effects, we have used customized prior probability maps during segmentation and included a correction for image non-uniformity.

To determine anatomical localization, SPM maps were overlayed onto a customized template which reflects the variance of structures. In doing so, it became apparent that the loss of grey matter in the occipital lobe area of PDD subjects was very close to the edge of the brain. Scalp, skull and fat on the inner surface of the skull in the occipital lobe are a problem during segmentation and can be classified wrongly. In an attempt to reduce these effects, we incorporated into our analyses an automated brain extraction step to clean up the grey matter segments and used customized templates to reduce bias. Nevertheless, it is possible that the occipital change could reflect inclusion of some non-brain structures in the Parkinson's disease group. In addition, VBM remains a relatively new analysis technique and we note the suggestion that atrophy detected in the deep grey matter nuclei in the PDD group may reflect misclassified voxels and interface shift due to ventricular enlargement (Good *et al*., 2001) in the patient group.

In PDD relative to DLB, we found no significant difference in the pattern of cerebral atrophy in either group. This strengthens the hypothesis that PDD is similar to DLB and might be part of the same disease spectrum. This is consistent with studies showing similarities in extrapyramidal motor features (Aarsland *et al*., 2001) and fluctuating attention (Ballard *et al*., 2002) in PDD and DLB.

Conclusion

We have demonstrated, using VBM, that Parkinson's disease involves grey matter loss in frontal areas. In PDD, this loss extends to the temporal, parietal and subcortical areas, with atrophy in the occipital lobe being the only difference between the two groups. Significantly, we have shown that atrophy of the temporal lobe, including the hippocampus and parahippocampal gyrus, is greater in Alzheimer's disease than in PDD. Using VBM, we have avoided the subjectivity associated with ROI based methods and have further demonstrated the use of automated whole brain analysis methods for the evaluation of brain structure in disease.

Acknowledgements

We wish to thank Elise Rowan for help with the database and Rachael Scahill for her help with the optimized VBM methods. This work was supported by a programme grant from the MRC.

References

Aarsland D, Anderseon K, Larsen JP, Lolk A, Nielsen H, Kragh-Sorensen P. Risk of dementia in Parkinson's disease. A community-based prospective study. Neurology 2001; 56: 730–6.

Aarsland D, Laake K, Larsen JP, Janvin C. Donepezil for cognitive impairment in Parkinson's disease: a randomised controlled study. J Neurol Neurosurg Psychiatry 2002; 72: 708–12.

Abe Y, Kachi T, Kato T, Arahata Y, Yamada T, Washimi Y, et al. Occipital hypoperfusion in Parkinson's disease without dementia: correlation to impaired cortical visual processing. J Neurol Neurosurg Psychiatry 2003; 74: 419–22.

Alegret M, Junque C, Pueyo R, Valleoriola F, Vendrell P, Tolosa E, et al. MRI atrophy parameters related to cognitive and motor impairment in Parkinson's disease. Neurologia 2001; 16: 63–9.

Antonini A, De Notaris R, Benti R, De Gaspari D, Pezzoli G. Perfusion ECD/SPECT in the characterization of cognitive deficits in Parkinson's disease. Neurol Sci 2001; 22: 45–6.

Apaydin H, Ahlskog JE, Parisi JE, Boeve BF, Dickson DW. Parkinson's disease neuropathology: later-developing dementia and loss of the levodopa response. Arch Neurol 2002; 59: 102–12.

Ashburner J, Friston KJ. Nonlinear spatial normalization using basis functions. Hum Brain Mapp 1999; 7: 254–66.

Ashburner J, Friston KJ. Voxel-based morphometry—the methods. Neuroimage 2000; 11: 805–21.

Ballard CG, Aarsland D, McKeith I, O'Brien J, Gray A, Cormack F, et al. Fluctuations in attention: Parkinson's disease dementia vs DLB with parkinsonism. Neurology 2002; 59: 1714–20.

Barber R, Ballard C, McKeith IG, Gholkar A, O'Brien JT. MRI volumetric study of dementia with Lewy bodies: a comparison with Alzheimer's disease and vascular dementia. Neurology 2000; 54: 1304–9.

Baron JC, Chetelat G, Desgranges B, Perchey G, Landeau B, de la Sayette V, et al. In vivo mapping of gray matter loss with voxel-based morphometry in mild Alzheimer's disease. Neuroimage 2001; 14: 298–309.

Brett M. The MNI brain and the Talairach atlas. MRC CBU Imaging home page. 1999. Available from: http: //www.mrc-cbu.cam.ac.uk/Imaging/contents.html

Burton EJ, Karas G, Paling SM, Barber R, Williams ED, Ballard CG, et al. Patterns of cerebral atrophy in dementia with Lewy bodies using voxel-based morphometry. Neuroimage 2002; 17: 618–30.

Camicioli R, Moore MM, Kinney A, Corbridge E, Glassberg K, Kaye JA. Parkinson's disease is associated with hippocampal atrophy. Mov Disord 2003; 18: 784–90.

Chan D, Fox NC, Jenkins R, Scahill RI, Crum WR, Rosser MN. Rates of global and regional cerebral atrophy in Alzheimer's disease and frontotemporal dementia. Neurology 2001; 57: 1756–63.

Chetelat G, Desgranges B, De La Sayette V, Viader F, Eustache F,

Baron J-C. Mapping gray matter loss with voxel-based morphometry in mild cognitive impairment. Neuroreport 2002; 13: 1939–43.

Colloby SJ, Fenwick JD, Williams ED, Paling SM, Lobotesis K, Ballard C, et al. A comparison of (99m)Tc-HMPAO SPET changes in dementia with Lewy bodies and Alzheimer's disease using statistical parametric mapping. Eur J Nucl Med Mol Imaging 2002; 29: 615–22.

Double KL, Halliday GM, McRitchie DA, Reid WG, Hely MA, Morris JG. Regional brain atrophy in idiopathic Parkinson's disease and diffuse lewy body disease. Dementia 1996; 7: 304–13.

Duda JE, Giasson BI, Mabon ME, Lee VM-Y, Trojanowski JQ. Novel antibodies to synuclein show abundant striatal pathology in Lewy body diseases. Ann Neurol 2002; 52: 205–10.

Fahn SRL, Elton RL, Marsden CD, Goldstein M. Unified Parkinson's disease rating scale. Recent developments in Parkinson's disease. Vol 2. London: Macmillan; 1987. p. 153–63.

Folstein MF, Folstein SE, McHugh PR. Mini-mental state. A practical method for grading the cognitive state of patients for the clinician. J Psychiatr Res 1975; 12: 189–98.

Friston KJ, Holmes AP, Worsley KJ, Poline J-P, Frith CD, Frackowiak RSJ. Statistical parametric maps in functional imaging: A general linear approach. Hum Brain Mapp 1995; 2: 189–210.

Galton CJ, Patterson K, Graham K, Lambon-Ralph MA, Williams G, Antoun N et al. Differing patterns of temporal atrophy in Alzheimer's disease and semantic dementia. Neurology 2001; 57: 216–25.

Gibb WRG, Lees AJ. The relevance of the Lewy body to the pathogenesis of idiopathic Parkinson's disease. J Neurol Neurosurg Psychiatry 1988; 5: 745–52.

Good CD, Johnsrude IS, Ashburner J, Henson RNA, Friston KJ, Frackowiak RSJ. A voxel-based morphometric study of ageing in 465 normal adult human brains. Neuroimage 2001; 14: 21–36.

Good CD, Scahill RI, Fox NC, Ashburner J, Friston KJ, Chan D, et al. Automatic differentiation of anatomical patterns in the human brain: validation with studies of degenerative dementias. Neuroimage 2002; 17: 29–46.

Hu MT, White SJ, Chaudhuri KR, Morris RG, Bydder GM, Brooks DJ. Correlating rates of cerebral atrophy in Parkinson's disease with measures of cognitive decline. J Neural Transm 2001; 108: 571–580.

Huber SJ, Shuttleworth EC, Christy JA, Chakeres DW, Curtain A, Paulson GW, et al. Magnetic resonance imaging in dementia of Parkinson's disease. J Neurol Neurosurg Psychiatry 1989; 52: 1221–7.

Karas BG, Burton EJ, Rombouts SARB, van Schijndel RA, O'Brien JT, Scheltens Ph, et al. A comprehensive study of gray matter loss in patients with Alzheimer's disease using optimized voxel-based morphometry. Neuroimage 2003; 18: 895–907.

Kassubek J, Juengling FD, Hellwig B, Spreer J, Lucking CH. Thalamic gray matter changes in unilateral parkinsonian resting tremor: a voxel-based morphometric analysis of 3-dimensional magnetic resonance imaging. Neurosci Lett 2002; 323: 29–32.

Laakso MP, Partanen K, Riekkinen P, Lehtovirta M, Helkala E-L, Hallikainen M, et al. Hippocampal volumes in Alzheimer's disease, Parkinson's disease with and without dementia, and in vascular dementia: an MRI study. Neurology 1996; 46: 678–81.

Lancaster JL, Woldorff MG, Parsons LM, Liotti M, Freitas CS, Rainey L, et al. Automated Talairach atlas labels for functional brain mapping. Hum Brain Mapp 2000; 10: 120–31.

McKeith IG, Galasko D, Kosaka K, Perry EK, Dickson DW, Hansen LA, et al. Consensus guidelines for the clinical and pathologic diagnosis of dementia with Lewy bodies (DLB): report of the consortium on DLB international workshop. Neurology 1996; 47: 1113–24.

McKeith IG, Ballard CG, Perry RH, Ince PG, O'Brien JT, Neill D, et al. Prospective validation of consensus criteria for the diagnosis of dementia with Lewy bodies. Neurology 2000; 54: 1050–8.

McKhann G, Drachman D, Folstein M, Katzman R, Price D, Stadlan EM. Clinical diagnosis of Alzheimer's disease: report of the NINCDS-ADRDA Work Group under the auspices of Department of Health and Human Services Task Force on Alzheimer's Disease. Neurology 1984; 34: 939–44.

Middelkoop HAM, van der Flier WM, Burton EJ, Lloyd AJ, Paling S, Barber R, et al. Dementia with Lewy bodies and Alzheimer's disease are not associated with occipital lobe atrophy on MRI. Neurology 2001; 57: 2117–20.

Mummery CJ, Patterson K, Price CJ, Ashburner J, Frackowiak RSJ, Hodges JR. A voxel-based morphometry study of semantic dementia: relationship between temporal lobe atrophy and semantic memory. Ann Neurol 2000; 47: 36–45.

O'Brien JT, Paling S, Barber R, Williams ED, Ballard C, McKeith IG, et al. Progressive brain atrophy on serial MRI in dementia with Lewy bodies, Alzheimer's disease, and vascular dementia. Neurology 2001; 56: 1386–8.

Owen AM, Doyon J. The cognitive neuropsychology of Parkinson's disease: a functional neuroimaging perspective. Adv Neurol 1999; 80: 49–56.

Reading PJ, Luce AK, McKeith IG. Rivastigmine in the treatment of parkinsonian psychosis and cognitive impairment: preliminary findings from an open trial. Mov Disord 2001; 16: 1171–4.

Riekkinen P Jr, Kejonen K, Laakso MP, Soininen H, Partanen K, Riekkinen M. Hippocampal atrophy is related to impaired memory, but not frontal functions in non-demented Parkinson's disease patients. Neuroreport 1998; 9: 1507–11.

Rombouts SA, Barkhof F, Witter MP, Scheltens P. Unbiased whole-brain analysis of gray matter loss in Alzheimer's disease. Neurosci Lett 2000; 285: 231–3.

Rosen HJ, Gorno-Tempini ML, Goldman WP, Perry RJ, Schuff N, Weiner M et al. Patterns of brain atrophy in frontotemporal dementia and semantic dementia. Neurology 2002; 58: 198–208.

Roth M, Tym E, Mountjoy CQ, Huppert FA, Hendrie H, Verma S, et al. CAMDEX A standardised instrument for the diagnosis of mental disorder in the elderly with special reference to the early detection of dementia. Br J Psychiatry 1986; 149: 698–709.

Rüb U, Del Tredici K, Schultz C, Ghebremedhin E, de Vos RAI, Jansen Steur E, et al. Parkinson's disease: the thalamic components of the limbic loop are severely impaired by α-synuclein immunopositive inclusion body pathology. Neurobiol Aging 2002; 23: 245–54.

Schulz JB, Skalej, M, Wedekind D, Luft AR, Abele M, Voigt K, et al. Magnetic resonance images-based volumetry differentiates idiopathic Parkinson's-syndrome from multiple system atrophy and progressive supranuclear palsy. Ann Neurol 1999; 45: 65–74.

Summerfield C, Gomez-Anson B, Tolosa E, Mercader J, Marti MJ, Pastor P, et al. Dementia in Parkinson's disease: a proton magnetic resonance spectroscopy study. Arch Neurol 2002; 59: 1415–20.

Talairach, J, Tournoux P. Co-planar stereotaxic atlas of the human brain. Stuttgart: Thieme; 1988.